PHYSICAL REVIEW B VOLUME 43, NUMBER 8 15 MARCH 1991-I

# Origin of the shear piezoresistance coefficient $\pi_{44}$ of $n$-type silicon

Yozo Kanda
*Hamamatsu University School of Medicine, Hamamatsu 431-31, Japan*

Katuhisa Suzuki
*Tokyo Metropolitan Institute of Technology, Hino, Tokyo 191, Japan*
(Received 6 August 1990)

It is shown that the origin of the shear piezoresistance (PR) coefficient $\pi_{44}$ of $n$-type silicon is a stress-induced effective-mass change of individual valleys rather than the stress-induced intervalley electron transfer, which has long been believed to be the dominant source of PR in many-valley semiconductors. An orthorhombic stress destroys the rotational symmetry of the ellipsoidal valleys and induces large effective-mass changes due to the special character of the conduction-band edge of silicon. The effective-mass anisotropy then leads to a transverse voltage when the current is along [100]. This mechanism predicts a sign and a magnitude of $\pi_{44}$ for $n$-type Si that are consistent with experiments hitherto known.

The piezoresistance effect of silicon and germanium was discovered by Smith many years ago.[1] Immediately following the discovery Herring[2] succeeded in explaining most of the observed features in $n$-type materials by an electron-transfer mechanism. This theory predicts the shear piezoresistance (PR) coefficient $\pi_{44}$ of $n$-type Si to vanish if the well-known conduction-band structure is assumed. The observed $\pi_{44}$ (Refs. 1, 3, and 4) is in fact small compared with other coefficients $\pi_{11}$ and $\pi_{12}$ but differs from zero beyond experimental error ($\pi_{44}=-13.6$, $\pi_{11}=-102.2$, $\pi_{12}=53.4$ in $10^{-11}$ $\text{Pa}^{-1}$).[1] It is the purpose of this Brief Report to present a solution to this long-standing puzzle.

We first recapitulate briefly the electron-transfer mechanism using the energy surface diagrams shown in Fig. 1. The solid lines show energy surfaces without stress and the dashed lines those with stress. The arrangement of Fig. 1(a) measures $\pi_{11}$ and $\pi_{12}$ when the current is parallel and perpendicular to the stress along $\langle 100\rangle$, respectively, and Fig. 1(b) measures $\pi_{44}$. Theoretical expressions for these[2,5-7] are

$$\pi_{11}=\frac{2\Xi_u}{3k_B\Theta}\frac{(s_{11}-s_{12})(1-L)}{1+2L}\ , \tag{1}$$

$$\pi_{12}=\frac{-\Xi_u}{3k_B\Theta}\frac{(s_{11}-s_{12})(1-L)}{1+2L}\ , \tag{2}$$

$$\pi_{44}=0\ , \tag{3}$$

in the electron-transfer theory, where $\Xi_u$ is the shear deformation potential, $s_{ij}$'s are the compliance constants, and $L=\mu_\perp/\mu_\parallel=m_\parallel\tau_\perp/m_\perp\tau_\parallel\equiv m_\parallel/m_\perp$. Here, $\mu$ is the mobility, $m$ is the effective mass, and the relaxation times are assumed as $\tau_\perp=\tau_\parallel$.

We consider the effect of strain on the electron effective mass which has been hitherto neglected. The conduction bands $\Delta_1$ and $\Delta_2'$ touch at the zone boundary $X$ point due to a special symmetry of the diamond structure, namely, the presence of a glide reflection plane. Hensel, Hasegawa, and Nakayama[8] considered the removal of this degeneracy by an external uniaxial stress and the consequent electron effective-mass shifts of $\Delta_1$ band due to strain mixing of the electronic wave functions. Under an orthorhombic strain $e_{xy}$ the electron ellipsoid will be distorted and the band energy becomes

$$E(\mathbf{k})=\frac{\hbar^2(k_z-k_0)^2}{2m_\parallel}+\frac{\hbar^2(k_x^2+k_y^2)}{2m_\perp}+\alpha\hbar^2e_{xy}k_xk_y\ , \tag{4}$$

where $\alpha=(86.8\pm5.0)/m$. We pay attention to the ellip-

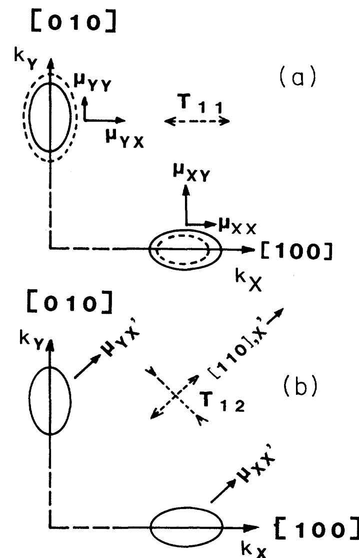


FIG. 1. Schematic diagram of the $\langle 100\rangle$ and $\langle 010\rangle$ valleys in $k$ space for $n$-type Si. Dashed lines show the effect of stress. (a) corresponds to $T_{11}$ stress and (b) to $T_{12}$.

 ©1991 The American Physical Society

soid on the $k_z$ axis. The cross section of the $k_z$ ellipsoid is shown schematically in Fig. 2(b). The energy surface is no longer an ellipsoid of revolution. Its cross section changes from a circle to an ellipse. On the other hand, the effective masses of the ⟨010⟩ and ⟨100⟩ ellipsoids are unaffected by $T_{12}$ stress.

Next, we will consider $\pi_{44}$. When a stress $T_{12}$ is applied to a four-terminal device whose current flows along ⟨100⟩, a transverse voltage which is proportional to $T_{12}$ is generated between the output electrodes because of asymmetry of the ⟨001⟩ effective mass to the ⟨100⟩ (current direction). The proportionality constant defines $\pi_{44}$,[9,10]

$$V_{\mathrm{out}}=\pi_{44} I T_{12} \tag{5}$$

or

$$\rho_{12}=\rho_0 \pi_{44} T_{12} , \tag{5'}$$

where $\rho_0$ is the isotropic resistivity of the unstressed crystal. The $\pi_{44}$ is given by

$$\pi_{44}=\frac{-a m_{\parallel} s_{44}}{1+2L} . \tag{6}$$

Conversely speaking, the effective-mass change with shear can be seen through the piezoresistance coefficient $\pi_{44}$ even at room temperature. From Eq. (6), $\pi_{44}$ is evaluated as $-9.4\times10^{-11}$ $\mathrm{Pa}^{-1}$ which agrees quite well with the experimental value by using the data $s_{44}=1.26\times10^{-11}$ $\mathrm{Pa}^{-1}$, $m_{\parallel}/m=0.9163$, $m_{\perp}/m=0.1905$. This case can be realized when the device is made in a Si square diaphragm under pressure at the position $T_x=-T_y$ or in a circular diaphragm under pressure at $T_r=-T_c$ where $T_r$ and $T_c$ are radial and circumferential stress, respectively.[11] The $\pi_{44}$ is identical to the difference between the longitudinal and the transverse piezoresistance coefficient under the ⟨110⟩ stress:

$$\pi_l\langle 110\rangle-\pi_t\langle 110\rangle=\pi_{44} . \tag{7}$$

A similar effect was detected in $N$-channel inversion layer metal-oxide-semiconductor (MOS) transistors.[12] In the case of the arrangement shown in Fig. 2(a), an isotropic mass shift occurs which was found to be an order of magnitude smaller than the anisotropic shift [arrangement of Fig. 2(b)] and is unimportant to the present discussion. Consequently, Eqs. (1) and (2) remain unchanged. Therefore the piezoresistance coefficients $\pi_{11}$, $\pi_{12}$, and $\pi_{44}$ in $n$-type Si can be expressed by Eqs. (1), (2), and (6), respectively. An isotropic mass change with shear stress $T_{12}$ which does not contribute to the transverse voltage was omitted in Eqs. (4) and (6). The $\pi_{44}$ is distinct from the $\pi_{11}$ and $\pi_{12}$ in temperature dependence. The former is independent of temperature while the latter is inversely proportional to absolute temperature.

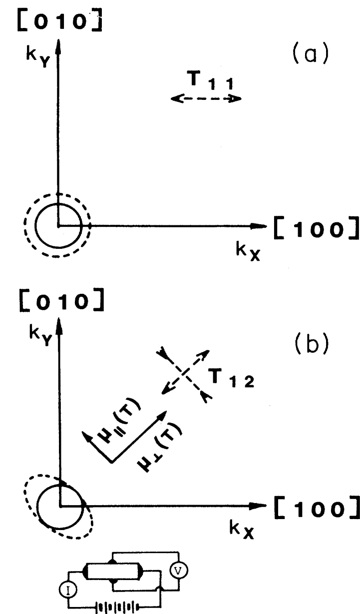


FIG. 2. Schematic diagram of the ⟨001⟩ valley in $k$ space for $n$-type Si. Dashed lines show the effect of stress. (a) corresponds to $T_{11}$ stress and (b) to $T_{12}$.

The piezoresistance effect in $n$-type Si can thus be explained by the electron-transfer mechanism and the effective-mass change in a way analogous to those in $p$-type Si.[13] Since the conduction band in germanium at the Brillouin-zone boundary (the $L$ point) is nondegenerate, the effective masses of the valleys do not change under shear stresses. From this reason, the piezoresistance effect in $n$-type Ge was explained more successfully by the electron-transfer mechanism.

There is a subsidiary contribution to PR as a result of the mean relaxation time through intervalley scattering because the density of final states depends on the relative position of the valleys in energy.[2,5,6] This contributes to $\pi_{11}$ and $\pi_{12}$ but not $\pi_{44}$.

We would like to thank Professor H. Hasegawa, Professor Y. Yasuda, Professor S. Zaima, T. Maruyama, and K. Matsuda for valuable discussions.

[1] C. S. Smith, Phys. Rev. **94**, 42 (1954).
[2] C. Herring, Bell Syst. Tech. J. **34**, 237 (1955).
[3] O. N. Tufte and E. L. Stelzer, Phys. Rev. **133**, A1705 (1964).
[4] K. Matsuda, Y. Kanda, and K. Suzuki, Jpn. J. Appl. Phys. **28**, L1676 (1989).
[5] C. Herring and E. Vogt, Phys. Rev. **101**, 944 (1956).
[6] R. W. Keyes, Solid State Phys. **11**, 149 (1960).
[7] Y. Kanda, IEEE Trans. Electron Devices **ED-29**, 64 (1982).
[8] J. C. Hensel, H. Hasegawa, and M. Nakayama, Phys. Rev. **138**, A225 (1965).
[9] W. G. Pfann and R. N. Thurston, J. Appl. Phys. **32**, 2008 (1961).

[10] Y. Kanda, Jpn. J. Appl. Phys. **26**, 1031 (1987).
[11] S. Timoshenko, *Theory of Plates and Shells* (McGraw-Hill, New York, 1940), p. 55.
[12] T. Maruyama, S. Zaima, Y. Koide, Y. Kanda, and Y. Yasuda, J. Appl. Phys. **68**, 5687 (1990).
[13] K. Suzuki, H. Hasegawa, and Y. Kanda, Jpn. J. Appl. Phys. **23**, L871 (1984).